

Structural mobility of molecular bottle-brushes investigated by NMR relaxation dynamics

Joanna Pietrasik¹, Brent S. Sumerlin², Hyung-il Lee, Roberto R. Gil, Krzysztof Matyjaszewski*

Center for Macromolecular Engineering, Department of Chemistry, Carnegie Mellon University, 4400 Fifth Avenue, Pittsburgh, PA 15213, United States

Received 28 October 2006; received in revised form 28 November 2006; accepted 28 November 2006

Available online 15 December 2006

Abstract

The structural mobility of monomeric units of molecular bottle-brushes was studied by a systematic evaluation of NMR relaxation dynamics. The spin–spin relaxation time (T_2) was determined by Carr–Purcell–Meiboom–Gill (CPMG) NMR spectroscopic measurements. T_2 for protons that reside on the exterior and interior of the bottle-brush macromolecules varied with the grafting density and side chain length in bottle-brush copolymers. Poly((2-(2-bromopropionyloxy)ethyl methacrylate-*stat*-methyl methacrylate)-*graft*-butyl acrylate) (poly((BPEM-*stat*-MMA)-*graft*-PBA) was studied as a model brush copolymer. The T_2 values for protons of MMA units in the brush backbone significantly decreased with increasing side chain length and grafting density of PBA. The mobility and relaxation times T_2 for the side chain PBA protons decreased with grafting density. However, after initial increase, the relaxation times eventually decreased with PBA side chain length.

© 2006 Elsevier Ltd. All rights reserved.

Keywords: Molecular bottle-brush; Graft copolymer; ATRP

1. Introduction

Bottle-brush polymers have extended cylindrical shapes [1–6]. The chain-extended conformation is the result of intramolecular excluded volume interactions, a consequence of the high grafting density along the backbone of the copolymer [7–9]. Therefore, variation in the grafting density along the backbone of the copolymer affects the conformations of the bottle-brush polymers. There are several reports that correlate the shape of the bottle-brush macromolecules to their architectural parameters [9–11]. Numerous techniques have been used to characterize the solution properties of bottle-brush molecules, including sedimentation velocity [12] and viscosity [13,14] measurements, dynamic light scattering

(DLS) [7,13,15], static light scattering (SLS) [13,15,16], small-angle neutron scattering (SANS) [17], and small-angle X-ray scattering (SAXS) [15,18].

Nuclear magnetic resonance has been extensively used to study the molecular dynamics of polymers in solution and in the solid state, since longitudinal (T_1) and transverse (T_2) relaxation times are extremely sensitive to chain motions.

In solution, the relaxation of polymers is caused by the combination of rapid vibrational motions, *gauche*–*trans* isomerization, and even slower segmental motions. Conformational transformations of melted or dissolved polymers are quite rapid as compared to the tumbling and looping motions of entire chains. These localized molecular motions are very effective in causing relaxation, and even for high molecular weight polymers, the reorientation of the entire chain makes only a small contribution to the overall relaxation [19–21].

Modeling the molecular dynamics of polymers in solution requires that the relaxation times of distinctive nuclear pairs (i.e. ^{13}C – ^1H) be measured in solution as a function of magnetic field strength and temperature and then compare the fits to various models. From these calculations, the motional correlation

* Corresponding author. Tel.: +1 412 268 3209; fax: +1 412 268 6897.

E-mail address: km3b@andrew.cmu.edu (K. Matyjaszewski).

¹ Present address: Institute of Polymer & Dye Technology, Department of Chemistry, Stefanowskiego 12/16, 90 – 924 Lodz, Poland.

² Present address: Department of Chemistry, Southern Methodist University, 3215 Daniel Avenue, Dallas, TX 75275-0314, United States.

times (τ_c) can be obtained, and in this way the solution relaxation of polymers has been extensively studied. By ^{13}C NMR studies, longitudinal relaxation times (T_1) and correlation times (τ_c) from a variety of polymers were calculated [22] using the isotropic correlation time model [23]. Although correlations obtained from this model are by no means quantitative, their gross trends led Bovey and Jelinski to postulate a series of conclusions about the dependence of chain mobility as a function of side chains, heteroatoms, double bonds and stereochemistry [22].

According to the Bloembergen–Purcell–Pound relaxation theory [24,25], at low correlation times (fast motion), $T_1 = T_2$. However, for higher correlation times (slower motion), T_1 differs from T_2 , and T_1 goes through a minimum, while T_2 decreases monotonically with correlation time. This trend is no longer valid near the rigid-lattice limit (solid state), i.e. when the correlation time $\tau_c > T_2$, since the spins dephase due to differences in resonance frequencies before relaxation due to motion. At the rigid-lattice limit, T_2 reaches an asymptotic limit where the relaxation behavior is far from being a single exponential [26–29]. These clear and predictable trends of the T_2 relaxation times as a function of molecular motion in the liquid state make it simple and convenient to monitor the local flexibility of polymeric segments as a function of their architecture [30–34]. Solid state transverse ^1H relaxation experiments have also been extensively used to characterize different aspects of the structure and dynamics of polymer chains, like cross-link density and chain dynamics of elastomeric materials [35–40] and polydimethylsiloxane (PDMS) grafted onto a silica surface [41], among other systems [19–21].

The aim of the current report is the qualitative correlation of architectural parameters of bottle-brush copolymers with the spin–spin relaxation time (T_2) of protons residing on the interior and exterior of bottle-brush macromolecules in solution. The ^1H transverse relaxation times (T_2) of each individual functional group in the brush molecules were measured using the Carr–Purcell–Meiboom–Gill (CPMG) pulse sequence [42–44] at 500 MHz with a liquid state probe. The trends of T_2 values were correlated with the brushes' architectural parameters such as grafting density and side chain length.

Atom transfer radical polymerization (ATRP) and other controlled radical polymerization (CRP) processes are suitable for the synthesis of molecular brushes since the low concentration of radicals present during the polymerizations reduces the contribution of inter- and intramolecular termination [45–47]. This is especially important for the preparation of brush macromolecules, due to the high concentration of chains that exist in the vicinity of the brush backbone and to the propensity for crosslinking when intermolecular termination occurs between multifunctional (co)polymers. As was demonstrated in previous studies, ATRP was successfully used for synthesizing brushes with different architectures, such as star-like multiarm structures [48–50], cylindrical brush–coil block copolymers [51,52], brushes with block copolymers as side chains [53–57], and brushes with a gradient in grafting density along the copolymer backbone [58–61]. In the current study, a series of bottle-brush polymers containing poly(*n*-butyl acrylate)

(PBA) side chains were synthesized by ATRP from poly(2-(2-bromopropionyloxy)ethyl methacrylate-*stat*-methyl methacrylate) with different compositions of methyl methacrylate (MMA) along the backbone of the copolymer. The grafting density was reduced by increasing the amount of MMA in the backbone. In addition to the grafting density, the length of the side chains was also systematically varied.

The synthesis of poly(2-(trimethylsilyloxy)ethyl methacrylate) (P(HEMA-TMS)) and poly(2-(2-bromopropionyloxy)ethyl methacrylate) (PBPEM) was previously reported [2]. To prepare P(BPEM-*stat*-MMA) macroinitiators, MMA was added to the reaction mixture as a comonomer in the polymerization of HEMA-TMS. The mol% of MMA in the mixture with HEMA-TMS was 78, 53 and 8. P((BPEM-*stat*-MMA)-*graft*-BA) (**B1-6**) and linear PBA (**L1**) were prepared as described below.

2. Experimental

2.1. Materials

All chemicals were purchased from Aldrich and used as received unless otherwise stated. Methyl methacrylate (MMA), *n*-butyl acrylate (BA, 99+%), and 2-(trimethylsilyloxy)ethyl methacrylate (HEMA-TMS, 99%) were distilled under vacuum prior to use. CuBr (98%) was purified by stirring with glacial acetic acid followed by filtering and washing the resulting solid with ethanol ($\times 3$) and diethyl ether ($\times 2$).

2.1.1. P((BPEM-*stat*-MMA)-*graft*-BA) (**B1**)

P(BPEM-*stat*-MMA) (0.100 g, 0.166 mmol BPEM-Br initiating sites, $M_n = 60,200$, $M_w/M_n = 1.10$, 22 mol% PBEM), CuBr₂ (99%) (0.001 g, 0.004 mmol), dNbpy (0.0686 g, 0.166 mmol), BA (8.5 g, 66.4 mmol), and anisole (5.0 mL) were added to a 25-mL Schlenk flask equipped with a magnetic stir bar. The flask was sealed, and the resulting solution was subjected to three freeze–pump–thaw cycles. After equilibration at room temperature, CuBr (0.012 g, 0.081 mmol) was added to the solution under nitrogen flow, and the flask was placed in an oil bath preheated to 70 °C. Aliquots were removed by syringe in order to monitor conversion and molecular weight evolution. After a predetermined time, the flask was removed from the oil bath and opened to expose the catalyst to air. The polymerization solution was diluted with CHCl₃ and passed over an alumina (activated neutral) column to remove the catalyst. Solvent was removed by rotary evaporation, and the polymer was isolated by precipitation into cold methanol. Several polymerizations were conducted under similar conditions using macroinitiators with different MMA contents and also with varying reaction times. This facilitated the determination of conversion by GC and gravimetry at various time intervals.

2.1.2. Linear PBA (**L1**)

For an analogous linear polymerization (**L1**), BA was polymerized under conditions similar to those employed for the synthesis of P((BPEM-*stat*-MMA)-*graft*-BA), except that

dimethyl 2,6-dibromoheptanedioate (DMDBrHD, 97%) was employed as a low molecular weight ATRP initiator.

2.2. Characterization

Monomer conversion was determined either by gravimetry or by a Shimadzu GC 14A gas chromatograph with a flame ionization detector and a J & W Scientific 30 m DB608 column (injector temp. = 250 °C; detector temp. = 250 °C; column initial temp. = 40 °C; heat ramp = 40 °C/min; column final temp. = 160 °C). The degree of functionalization of the macroinitiator was determined by ¹H NMR spectroscopy in CDCl₃ with a Bruker Avance DMX-500 spectrometer operating at 500.13 MHz. Apparent molecular weights were determined by GPC (Waters Microstyrigel columns (guard, 10⁵, 10³, and 10² Å), THF eluent at 35 °C, flow rate = 1.00 mL/min). GPC molecular weights were evaluated with a calibration based on linear poly(methyl methacrylate) (PMMA) for the backbone and linear polystyrene for the molecular brushes. *T*₂ NMR measurements were recorded in a Bruker Avance DMX-500, using a liquid state BBI probe with Z-gradients. Measurements were performed as discussed in the paper. Concentration of the polymer solutions in chloroform used for the *T*₂ NMR measurements was ~0.02 mg/μL. The experimental error estimated from the signal to noise ratio and the experiment repetition were ±5%.

3. Results and discussion

3.1. Brush syntheses

The general conditions for the brush syntheses are listed in Table 1. The molecular weight distributions remained

Table 1
Results from polymerizations of *n*-butyl acrylate (BA) as linear chains and from a poly(2-(2-bromopropionyloxy)ethyl methacrylate-*stat*-methyl methacrylate) with varying copolymer composition

Sample	Grafting density (mol% BPPEM)	Conv _{SC} ^a (%)	DP _{SC} ^b	<i>M</i> _{n,th}	<i>M</i> _{n,GPC}	<i>M</i> _w / <i>M</i> _n
B1 ^c	22	2.5	10	184,000	115,000	1.10
B2 ^c	22	3.4	17	271,000	220,000	1.15
B3 ^c	22	10.5	42	582,000	322,600	1.13
B4 ^c	22	16.0	89	1,170,000	453,000	1.22
B5 ^d	47	6.4	29	642,000	265,000	1.14
B6 ^e	92	5.1	23	820,000	320,000	1.15
L1	—	—	42	5400	5700	1.15

Conv_{SC} – monomer conversion during PBA side chains synthesis, DP_{SC} – degree of polymerization of PBA side chains.

^a Determined by gravimetry or gas chromatography.

^b Calculated from DP_{SC,th} = ([BA]/[BPPEM-Br]) × conversion. **B1**: [BA]:[BPPEM-Br]:[CuBr]:[CuBr₂]:[dNbpy] = 400:1:0.5:0.025:1.05 at *T* = 70 °C with 100 vol% anisole; **B2, B4**: [BA]:[BPPEM-Br]:[CuBr]:[CuBr₂]:[dNbpy] = 554:1:0.7:0.035:1.47 at *T* = 70 °C with 4 vol% MEK; **B3, B5, B6**: [BA]:[BPPEM-Br]:[CuBr]:[CuBr₂]:[dNbpy] = 400:1:0.5:0.025:1.05 at *T* = 70 °C with 4 vol% MEK; **L1**: [BA]:[DMDBrHD]:[CuBr]:[PMDETA] = 60:1:0.5:0.5 at 70 °C with 10 vol% anisole.

^c Macroinitiator: *M*_n = 60,200, *M*_w/*M*_n = 1.10.

^d Macroinitiator: *M*_n = 65,400, *M*_w/*M*_n = 1.10.

^e Macroinitiator: *M*_n = 77,200, *M*_w/*M*_n = 1.17.

relatively narrow throughout the polymerizations. The absolute molecular weights are significantly higher than that measured from GPC using linear standards. The previous MALLS and AFM analyses indicate that the molecular brushes should have molecular weights very close to the theoretical values calculated on the basis of conversion of BA and concentration of the backbone [62].

3.2. General *T*₂ measurements for PBPEM macroinitiator and PBA brushes

All ¹H NMR spectroscopic experiments were conducted on a Bruker Avance DMX-500 spectrometer operating at 500.13 MHz using a liquid state BBI probe with Z-gradients. All measurements were performed in CDCl₃ solution at 300 K. During all measurements, the spinner was off. *T*₂ NMR measurements were recorded using the standard CPMG pulse sequence ((π/2)_X – τ – π_Y – 2τ – π_Y – 2τ – π_Y – ...) from the Bruker software library [43]. Spectra were collected in pseudo-2D mode: high-resolution chemical shifts in the F2 dimension and *T*₂ decays in the F1 dimension, as shown in Fig. 1. Measurements were obtained for each samples using the following parameters: 90° – pulse width (8.4 μs), echo delay D20 (1 ms) to prevent error due to translational diffusion, recycle delay (10 s), time domain TD (16 K), acquisition time (1.36 s), variable delay list of 50 points, sampling from 0.004 s to 3.0 s. In order to calculate the *T*₂ values, the peak intensity of each individual decay was fitted to a single exponential, since the experiments were carried out in solution where the molecular motion is isotropic and chemical shift-related artifacts do not occur. *T*₂ fits were performed using the Bruker relaxation analysis routine within the XWINNMR 3.5 software.

The aforementioned conditions were chosen because *T*₂ is generally more difficult to measure than *T*₁. The simplified method of determining *T*₂ is by varying τ in the standard

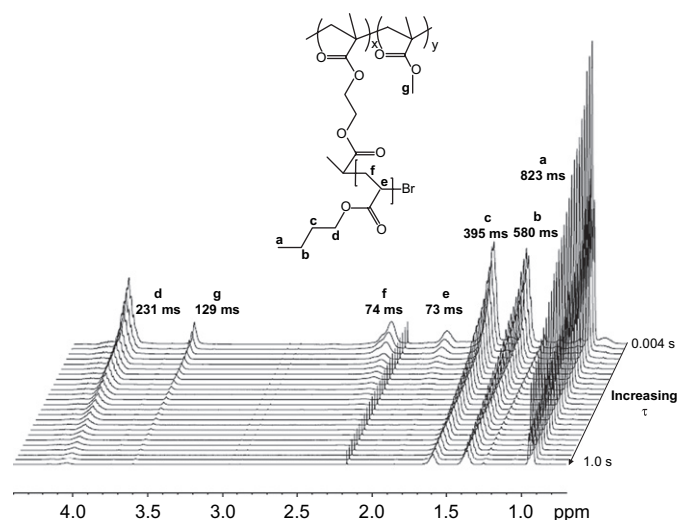


Fig. 1. ¹H NMR spectra of poly((BPPEM-*stat*-MMA)-graft-BA) brush molecule (**B2**), grafting density: 22 mol% BPPEM, DP_{SC} = 17, *M*_{n,GPC} = 220,000, *M*_w/*M*_n = 1.15 as a function of delay time (τ). Some spectra from the CPMG experiments obtained at the τ increments are omitted for clarity.

spin echo experiment then measuring the decay of the echo amplitudes. However, this method is not generally efficient, especially for long values of T_2 . There are also some problems with this method in solution. T_2 is independent of any inhomogeneities in the magnetic field, however, T_2^* is the field dependent time constant. Because of this, molecules should not diffuse during the experiment. For the echo to work properly, the speed of individual vectors must be the same before and after the 180° pulse, and this is not true if the molecular diffusion is significant. This is a more important problem at long values of τ . Spinning the sample can also interfere with measurements of T_2 as molecules are promoted to move in the magnetic field during the experiment. Hence, spinning is generally turned off, or the rate is slow as compared to the values of T_2 . Finally, π pulses are always a problem due to off-resonance effects and incorrect calibration. The 180° flip must be exact or the experiment fails. These are the reasons why we decided to use the CPMG pulse sequence, which to some extent corrects for the errors mentioned above.

The ^1H NMR spectra with peak assignments of poly((BPEM-*stat*-MMA)-*graft*-BA) molecular brush (**B2**) with $\text{DP}_{\text{SC}} = 17$ ($M_{n,\text{GPC}} = 220,000$; $M_w/M_n = 1.15$, 22 mol% BPEM) synthesized from the backbone with MMA content 78 mol% ($M_n = 60,200$; $M_w/M_n = 1.10$) are shown in Fig. 1 as a function of delay time (τ). Calculated T_2 values for peaks *a*–*g* are directly illustrated in Fig. 1 and shown in Table 2 for comparison. The degree of functionalization of the macroinitiator was determined by ^1H NMR.

As expected, the changes in intensity as a function of τ depend on the proton environment (peaks *a*–*d*). The following comparisons are qualitative, and although the T_2 values are from different functional groups, they show an interesting trend that is also related to the mobility of the different fragments. The T_2 values range from 823 ms for peak *a* (methyl of *n*-butyl chain) to 231 ms for peak *d* (methylene adjacent to ester oxygen). The two methylene units in the middle of the *n*-butyl chain (*b* and *c*) have similar T_2 values, and the resonances *e* and *f* show values of 73 and 74 ms, respectively. As noted below, all of these values are different from those measured for linear PBA chains (**L1**, Table 2). The methoxy groups of the MMA units in the interior of the brush (*g*) are excellent probes to monitor backbone mobility. In sample

B2, the backbone protons are densely surrounded by PBA side chains and therefore relax very quickly with $T_2 = 128$ ms. This value can be compared to $T_2 = 226$ ms for the same protons in the poly(BPEM-*stat*-MMA) macroinitiator with no side chains attached (Table 2). This difference in the T_2 values is evidence for the congested environment on the interior of the molecular brush.

The most common mechanism of relaxation in liquids is a result of dipole–dipole interactions between proton spins and their averaging due to molecular motion. As opposed to ^{13}C NMR spectroscopy in which bound protons dominate the dipole–dipole interactions with carbon, in ^1H NMR spectroscopy, proton dipole–dipole interactions with each nearby proton is the predominant relaxation process. Hence, T_2 relaxation rates will depend on the proton–proton distances and on the number of proton dipole–dipole interactions. Because of these factors, the comparison of T_2 values for functional groups in different chemical environments in relation to molecular mobility is not straightforward. Therefore, the comparison of T_2 values for the protons of molecular brushes as a function of grafting density and side chain length was between identical functional groups. Nonetheless, the significant difference in T_2 values observed between protons belonging to different groups in the backbone and side chains is likely not only the effect of differences in chemical environment but also to significant differences in mobility (Table 2). In most of the cases, a gross difference of one order of magnitude in the T_2 values between the inner and the outer protons of the brushes was observed. Although, in different time scales (liquid vs solid state), these results are comparable to those reported for PDMS chains attached to silica surfaces in which the segments adjacent to the surface had a $T_2^{\text{in}} \sim 0.08$ ms, and more mobile segments further from the interface had a $T_2^{\text{mo}} \sim 1$ – 3 ms [41], where a difference of one order of magnitude for the T_2 values was similarly observed.

3.3. Effect of side chain length

Polymer brushes containing PBA side chains with different degrees of polymerization (DP_{SC}) were synthesized from one poly(BPEM-*stat*-MMA) macroinitiator containing 78 mol% of MMA. DP_{SC} was varied from 10 to 90. Table 2 contains the

Table 2

T_2 values of protons of poly[(BPEM-*stat*-MMA)-*graft*-BA] brushes with different DP of the PBA side chains and different grafting densities of the copolymer brushes

DP_{SC}	Grafting density (mol% BPEM)	T_2 (ms)						
		<i>a</i>	<i>b</i>	<i>c</i>	<i>d</i>	<i>e</i>	<i>f</i>	<i>g</i>
0 (BPEM)	22	–	–	–	–	–	–	226
10 (B1)	22	651	453	337	194	86	50	152
17 (B2)	22	823	580	395	231	73	74	129
42 (B3)	22	897	654	446	215	78	71	95
89 (B4)	22	716	500	343	188	61	69	64
42	0 (L1)	1042	780	453	394	113	117	–
17	22 (B2)	823	580	395	231	73	74	129
29	47 (B5)	680	491	336	209	63	75	41
23	92 (B6)	660	468	116	188	59	67	–

T_2 values for methoxy protons from MMA units in the backbone (g) and side chain protons of BA units ($a-f$). A significant decrease in the T_2 values for protons from MMA units in the backbone (g) ranging from 152 ms for $DP_{SC} = 10$ to 64 ms for $DP_{SC} = 89$ was observed. As might be expected, the molecular constraint in the vicinity of the backbone increased with the molecular weight of the side chains.

The peaks of the n -butyl groups of the side chains relax in a more complex way. When the DP of the PBA side chains was increased from 10 to 42, T_2 values for most of the protons ($a-f$) increased. However, when the side chain length was further increased to $DP_{SC} = 89$, a decrease in the composite T_2 values was noted. A similar trend was previously reported by Vega et al. [39] for the T_2 values of PDMS networks as a function of molecular weight in solid state NMR. It is well known that the longer the amplitude and/or the frequency of chain motions, the higher the T_2 value [41]. As the length of the PBA side chains increases, the amplitudes of the chain oscillations increase, resulting in larger T_2 values until a certain range of DP_{SC} is reached. Eventually, the interactions between longer side chains, due to excluded volume effects, may reduce side chain mobility and enhance spin–spin relaxation rates, resulting in a lower T_2 value. Although the increment in PBA side chain length increases the molecular weight of the brushes, leading to an increase in the overall molecular correlation time, we do not think this causes the above behavior, since the overall reorientation of the entire chain makes only a small contribution to the relaxation, as previously described.

Fig. 2 illustrates the change in relaxation times for the protons from the brush backbone (g) and side chains (arbitrarily chosen c protons from PBA side chains) with different DP_{SC} .

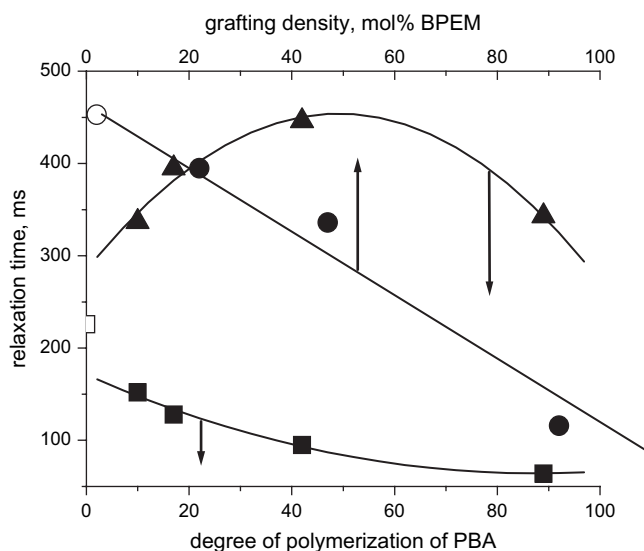


Fig. 2. T_2 relaxation times of g MMA protons from the backbone (■, DP_{SC} varied, grafting density: 22 mol% BPEM) and c protons from the PBA side chains (average values) (▲, DP_{SC} varied, grafting density: 22 mol% BPEM) (●, grafting density varied, $DP_{SC} = 23 \pm 6$) of the brush molecules. Empty symbols correspond to the backbone (□, $DP_{SC} = 0$) and linear PBA (○, grafting density = 0).

3.4. Effect of grafting density

Molecular brushes with different grafting densities were studied. The backbones with the low grafting density were prepared by copolymerization of two methacrylates (MMA and HEMA-TMS) with similar reactivity ratios (~ 1). Thus, the backbone grafting density was uniform and corresponded to the feed ratio. The interior and exterior parts of the bottle-brushes were investigated by measuring the T_2 values of the MMA backbone units and PBA side chains and also by the comparison to linear PBA.

Higher grafting density increased steric congestion and affected the mobility of g protons in the interior portions of the brushes. Therefore, the T_2 values were lower for the brush with higher grafting density (B5). Unfortunately, the signals from the MMA units were not detectable for the molecular brush with 92 mol% of BPEM, (B6) (Table 2, not shown in Fig. 2).

Grafting density also affected the T_2 values of the side chains (Table 2). Fig. 2 shows the continuous decrease in relaxation times with grafting density for c protons from PBA, for which this trend was most visible. T_2 values decreased from 395 ms for 22% grafting density to 116 ms for 92% grafting density. This indicates the progressive loss of mobility of side chains upon congestion due to higher local chain densities. For comparison, linear PBA was also studied, and the T_2 values for c protons were only slightly higher (453 ms) than those for the brush with 22% grafting density, which indicates that the side chains of the loosely grafted brush relax in a similar manner to free linear chains.

4. Conclusions

T_2 measurements using the CPMG NMR pulse sequence give significant insight into the organization and structure of molecular brushes in solution. The analysis of spin–spin relaxation times for protons in different locations throughout the brushes provided information on local molecular mobility. T_2 values for MMA units in the core of the brushes strongly decrease with increasing grafting density and side chain length. The average T_2 values for the side chains decrease with grafting density, and after an initial increase, a reduction in T_2 was observed for longer side chain lengths. T_2 measurements support the concept of high molecular congestion on the interior of bottle-brushes and may provide insight into local environments of other highly congested polymeric systems.

Acknowledgments

This work was supported by the National Science Foundation (DMR 05-49355), Kosciuszko Foundation and CRP Consortium at CMU. The NMR spectrometers of the Department of Chemistry NMR Facility at Carnegie Mellon University were purchased in part with funds from the National Foundation of Sciences (CHE-0130903).

References

- [1] Zhang M, Mueller AHE. *J Polym Sci Part A Polym Chem* 2005;43:3461.
- [2] Beers KL, Gaynor SG, Matyjaszewski K, Sheiko SS, Moeller M. *Macromolecules* 1998;31:9413.
- [3] Dziezok P, Sheiko SS, Fischer K, Schmidt M, Moller M. *Angew Chem Int Ed* 1997;36:2812.
- [4] Sheiko SS, Moller M. *Chem Rev* 2001;101:4099.
- [5] Sumerlin BS, Neugebauer D, Matyjaszewski K. *Macromolecules* 2005;38:702.
- [6] Sheiko SS, Sun F, Randall A, Shirvanyants D, Rubinstein M, Lee H-i, et al. *Nature* 2006;440:191.
- [7] Fischer K, Schmidt M. *Macromol Rapid Commun* 2001;22:787.
- [8] Sun F, Sheiko SS, Moeller M, Beers K, Matyjaszewski K. *J Phys Chem A* 2004;108:9682.
- [9] Rathgeber S, Pakula T, Wilk A, Matyjaszewski K, Beers KL. *J Chem Phys* 2005;122:124904.
- [10] Elli S, Ganazzoli F, Timoshenko FG, Kuznetsov YA, Connolly R. *J Chem Phys* 2004;120:6257.
- [11] Feuz L, Leermakers FAM, Textor M, Borisov O. *Macromolecules* 2005;38:8891.
- [12] Nemoto N, Nagai M, Koike A, Okada S. *Macromolecules* 1995;28:3854.
- [13] Wintermantel M, Schmidt M, Tsukahara Y, Kajiwara K, Kohjiya S. *Macromol Rapid Commun* 1994;15:279.
- [14] Tsukahara Y, Kohjiya S, Tsutsumi K, Okamoto Y. *Macromolecules* 1994;27:1662.
- [15] Wintermantel M, Gerle M, Fischer K, Schmidt M, Wataoka I, Urakawa H, et al. *Macromolecules* 1996;29:978.
- [16] Terao K, Nakamura Y, Norisuye T. *Macromolecules* 1999;32:711.
- [17] Lecommandoux S, Checot F, Borsali R, Schappacher M, Deffieux A, Brulet A, et al. *Macromolecules* 2002;35:8878.
- [18] Wataoka I, Urakawa H, Kobayashi K, Akaike T, Schmidt M, Kajiwara K. *Macromolecules* 1999;32:1816.
- [19] Bovey FA, Mirau PA. *NMR of polymers*. San Diego: Academic Press; 1996.
- [20] Ibbett RN. *NMR spectroscopy of polymers*. London, New York: Blackie Academic & Professional; 1993.
- [21] Mirau PA. *A practical guide to understanding the NMR of polymers*. New Jersey: John Wiley & Sons; 2004.
- [22] Bovey FA, Jelinski LW. *J Phys Chem* 1985;89:571.
- [23] Heatley F. *Prog Nucl Magn Reson Spectrosc* 1979;13:47.
- [24] Bloembergen N, Purcell EM, Pound RV. *Phys Rev* 1948;73:679.
- [25] Kubo R, Tomita K. *J Phys Soc Jpn* 1954;9:888.
- [26] Saalwaechter K, Herrero B, Lopez-Manchado MA. *Macromolecules* 2005;38:9650.
- [27] Saalwaechter K, Herrero B, Lopez-Manchado MA. *Macromolecules* 2005;38:4040.
- [28] Saalwaechter K. *Macromolecules* 2005;38:1508.
- [29] Brereton MG. *Macromolecules* 1990;23:1119.
- [30] Poe GD, Jarrett WL, Scales CW, McCormick CL. *Macromolecules* 2004;37:2603.
- [31] Convertine AJ, Lokitz BS, Vasileva Y, Myrick LJ, Scales CW, Lowe AB, et al. *Macromolecules* 2006;39:1724.
- [32] Assink RA, Celina M, Minier LM. *J Appl Polym Sci* 2002;86:3636.
- [33] Charlesby A. *Radiat Phys Chem* 1992;39:45.
- [34] Duncan DC, Whitten DG. *Langmuir* 2000;16:6445.
- [35] Litvinov VM, De PP. *Spectroscopy of rubber and rubbery materials*. Shropshire: Rapra Technology; 2002.
- [36] Simon G, Baumann K, Gronski W. *Macromolecules* 1992;25:3624.
- [37] Simon G, Schneider H. *Makromol Chem Macromol Symp* 1991;52:233.
- [38] Gronski W, Hoffmann W, Simon G, Wutzler A, Straube E. *Rubber Chem Technol* 1992;65:63.
- [39] Vega DA, Villar MA, Valles EM, Steren CA, Monti GA. *Macromolecules* 2001;34:283.
- [40] Steren CA, Monti GA, Marzocca AJ, Cerveny S. *Macromolecules* 2004;37:5624.
- [41] Litvinov VM, Barthel H, Weis J. *Macromolecules* 2002;35:4356.
- [42] Carr HY, Purcell EM. *Phys Rev* 1954;94:630.
- [43] Meiboom S, Gill D. *Rev Sci Instrum* 1958;29:688.
- [44] Claridge T, editor. *High-resolution NMR techniques in organic chemistry*. New York: Pergamon; 2000.
- [45] Matyjaszewski K, Xia J. *Chem Rev* 2001;101:2921.
- [46] Wang JS, Matyjaszewski K. *J Am Chem Soc* 1995;117:5614.
- [47] Goto A, Fukuda T. *Prog Polym Sci* 2004;29:329.
- [48] Matyjaszewski K. *Polym Int* 2003;52:1559.
- [49] Matyjaszewski K, Qin S, Boyce JR, Shirvanyants D, Sheiko SS. *Macromolecules* 2003;36:1843.
- [50] Boyce JR, Shirvanyants D, Sheiko SS, Ivanov DA, Qin S, Boerner H, et al. *Langmuir* 2004;20:6005.
- [51] Khelfallah N, Gunari N, Fischer K, Gkogkas G, Hadjichristidis N, Schmidt M. *Macromol Rapid Commun* 2005;26:1693.
- [52] Qin S, Matyjaszewski K, Xu H, Sheiko SS. *Macromolecules* 2003;36:605.
- [53] Boerner HG, Beers K, Matyjaszewski K, Sheiko SS, Moeller M. *Macromolecules* 2001;34:4375.
- [54] Zhang M, Breiner T, Mori H, Muller AHE. *Polymer* 2003;44:1449.
- [55] Cheng G, Boeker A, Zhang M, Krausch G, Mueller AHE. *Macromolecules* 2001;34:6883.
- [56] Lee H-i, Pietrasik J, Matyjaszewski K. *Macromolecules* 2006;39:3914.
- [57] Lee H, Jakubowski W, Matyjaszewski K, Yu S, Sheiko SS. *Macromolecules* 2006;39:4983.
- [58] Matyjaszewski K, Ziegler MJ, Arehart SV, Greszta D, Pakula T. *J Phys Org Chem* 2000;13:775.
- [59] Boerner HG, Duran D, Matyjaszewski K, da Silva M, Sheiko SS. *Macromolecules* 2002;35:3387.
- [60] Lord SJ, Sheiko SS, LaRue I, Lee H-i, Matyjaszewski K. *Macromolecules* 2004;37:4235.
- [61] Lee H-i, Matyjaszewski K, Yu S, Sheiko SS. *Macromolecules* 2005;38:8264.
- [62] Sheiko SS, da Silva M, Shirvanians D, LaRue I, Prokhorova S, Moeller M, et al. *J Am Chem Soc* 2003;125:6725.